

Enhanced Cascade Refrigeration System Performance via Fuzzy-Based Multi-Objective Optimization

Mohamed A. Atef¹, Shazly M. Salem², Mostafa H. Hussein^{3*}

¹ Process Department, Thyssenkrupp Uhde, Egypt

² Chemical and Petroleum Refining Engineering Department, Faculty of Petroleum and Mining Engineering – Suez University- Suez 41522 – Egypt

³ Chemical Engineering Department, Higher Institute of Engineering – Shorouk Academy- Shorouk City 11837 – Cairo – Egypt

Received October 19, 2024; Accepted February 6, 2025

Abstract

Refrigeration cycles are indispensable for processes operating below ambient temperatures, predominantly relying on vapor-recompression systems. This study introduces a computational model grounded in energy and exergy analyses aimed at synthesizing cascade refrigeration systems. The principal objectives include maximizing the coefficient of performance (COP), minimizing compressor power input, and optimizing refrigerant flow rates. To achieve these goals, a novel multi-objective optimization approach employing fuzzy analogical gates is proposed. This strategy utilizes a sequence of symmetric AND gates followed by asymmetric Invoke gates, strategically optimizing weight index selections. Cascade refrigeration systems encompass two or more distinct refrigeration circuits: the Low Temperature Circuit (LTc) and the High Temperature Circuit (HTc). These circuits are interconnected through a cascade heat exchanger, facilitating the transfer of heat from the (LTc) condenser to the (HTc) evaporator. A critical focus lies in achieving an optimal temperature differential within the cascade heat exchanger to enhance overall system efficiency. To validate the practical applicability of this methodology, two case studies involving configurations with two and three refrigeration cycles were conducted. The findings underscore the cost-effectiveness of the proposed approach compared to conventional methodologies, demonstrating substantial enhancements in system performance and energy efficiency. By leveraging advanced optimization techniques and rigorous thermodynamic analyses, this study contributes to advancing the design and operation of cascade refrigeration systems. The integration of fuzzy analogical gates not only enhances decision-making processes but also offers a pathway towards achieving more sustainable and economically viable refrigeration solutions for industrial applications.

Keywords: Cascade refrigeration; Cost, Multi-objective optimization; Fuzzy Analogical gates; Three-stage cascade refrigeration system; Refrigerant.

1. Introduction

Refrigeration systems play a crucial role in the chemical and petrochemical process industries, influencing product quality, energy efficiency, and overall plant profitability. Among the various configurations available, cascade refrigeration systems stand out for their ability to deliver superior performance through the efficient utilization of multiple refrigeration stages. The primary goal of synthesizing cascade refrigeration systems is to minimize total energy consumption during operation. This objective encompasses optimizing compressor work and reducing energy losses across different unit operations. In a typical vapor compression system, which includes components such as evaporators, compressors, condensers, and expansion valves, external energy is supplied to the compressor. Heat is absorbed in the evaporator, and heat rejection occurs in the condenser. Cascade refrigeration systems address the need for achieving lower temperatures, typically ranging from -90 to -30°C, which are crucial in

various industrial processes. These systems operate using two separate refrigeration cycles with different refrigerants: typically, NH_3 in the (HTc) and CO_2 in the (LTc). The effectiveness of cascade systems hinges significantly on identifying an optimal intermediate temperature, which serves as either the condensation temperature of the (LTc) or the evaporation temperature of the (HTc). This optimization is pivotal for maximizing overall system efficiency. The core objective of this study is to conduct multi-objective optimization, focusing on maximizing the coefficient of performance (COP), minimizing power consumption, and optimizing the flow rate within the refrigeration cycle. Achieving these objectives not only enhances the energy efficiency of cascade refrigeration systems but also contributes to cost savings and environmental sustainability in industrial operations. By integrating advanced optimization techniques and considering the thermodynamic properties of the refrigerants used in cascade systems, researchers and engineers aim to refine system design and operation. This approach ensures that cascade refrigeration systems meet the stringent performance demands of modern industrial processes while adhering to sustainability goals. In conclusion, cascade refrigeration systems represent a sophisticated solution for achieving precise temperature control in industrial applications. Their design and optimization play a pivotal role in enhancing energy efficiency, reducing operational costs, and ultimately, improving the overall competitiveness and sustainability of chemical and petrochemical process industries. Future research efforts will continue to focus on refining these systems to meet evolving industrial needs and environmental standards.

2. Literature review

Early research on the optimal design of cascade refrigeration systems focused on heuristic methods. Barnes and King [1] pioneered this field, proposing a preliminary model and heuristic rules for initial design and optimization. Cheng and Mah [2] expanded upon this work, introducing an interactive approach that employed evolutionary rules to refine the initial structure and extend the system to mixed refrigerants. However, these methods, relying heavily on heuristics, were unable to guarantee optimal solutions for complex systems.

Zhang and Xu [3] offered a more comprehensive approach to the synthesis of cascade refrigeration systems. They utilized exergy analysis and temperature-based charts to gain a deeper understanding of thermodynamic performance. This analysis provided a strong foundation for both conceptual design and system retrofitting. Furthermore, they developed a (MINLP) model to improve the synthesis of multi-level cascade refrigeration systems.

Ha Dinh *et al.* [4] also developed a comprehensive methodology for cascade refrigeration system synthesis. Their approach included exergetic analysis, optimization modelling, heat exchanger configuration identification, and rigorous simulation-based validation. They minimized the total compressor shaft work of the (HEN) by introducing a mathematical model.

Building upon multi-objective optimization, Saeed Eini *et al.* [5] evaluated cascade refrigeration systems from economic, exergetic, and environmental perspectives, as well as considering inherent safety. Their economic objective function encompassed capital, processing, and social costs. They also incorporated exergetic efficiency and quantitative risk assessment to calculate the total risk level. Decision analysis approaches were employed to determine the final optimal solution.

Danleichen *et al.* [6] focused on the simultaneous design of refrigeration sequences and (HENs), formulating the synthesis as a (GDP) problem. Their goal was to minimize total mechanical work of the compressor shaft. They improved a superstructure to determine optimal pressure levels, sub cooler configurations, total flow rate, and (HEN) structure. The superstructure included sub coolers and expansion valves connected in series to decrease inlet temperatures and energy consumption. A (GDP) was used to handle process variables, and (MINLP) based models were devised to facilitate optimal synthesis.

Roy and Kumarmandal [7] analyzed the influence of multiple design factors affecting the coefficient of performance, exergy efficiency, economic and environmental performance, and overall system cost rate for refrigerant combinations. Using a GA for multi-objective optimization, they evaluated different refrigerant pairs to achieve optimal performance, maximizing

exergy efficiency while reducing the overall cost rate of the plant and its associated operating conditions.

Danleichen [8] further explored optimization techniques, presenting a study on the simultaneous enhancement of refrigeration systems and their HEN applying a de-redundant model and a (PSO) algorithm. To address the challenges of large-scale non-convex (MINLP) problems, the research proposed an optimization framework that enhanced the solution space while managing computational complexity. A comprehensive and compact model with a tandem arrangement of sub-coolers and expansion valves was used to optimize pressure and temperature levels. The "two-step transformation method" transformed the cross-level arrangement into a non-cross-level configuration, resulting in a de-redundant superstructure. Case studies involving ethylene and propylene refrigeration systems demonstrated improved optimal outcomes with reduced computational time compared to conventional approaches.

Martinelli [9] adopted an integrated approach to the simultaneous synthesis and optimization of refrigeration cycles and their HEN. His work aimed to determine the economically optimal configuration of the refrigeration cycle, including factors such as the number of evaporation/condensation levels, compressor intercooling, and multiple throttling. A novel refrigeration cycle superstructure and an efficient solution algorithm based on problem decomposition were key features. Application to case studies demonstrated significantly improved efficiency and economic performance compared to previous studies. The computational tractability of the proposed approach was highlighted, making it applicable to real-world industrial scenarios.

Finally, Danleichen [10] explored the synthesis of cascade refrigeration systems (CRS) using a hybrid (SA) and (PSO) algorithm. These systems offer a broader range of refrigeration temperature options and higher energy efficiency compared to single- fluid refrigeration systems. The research proposed a randomized optimization approach for the synthesis of (CRS), formulating a (MINLP) model that incorporates a newly developed framework. The proposed optimization structure applied an (SA) algorithm to adjust the number of pressure and temperature levels in all sub refrigeration systems, while a (PSO) algorithm handled the optimization of continuous variables. A research case focusing on CRS optimization within an ethylene generation site showcased the method's effectiveness, leading to a significant decrease in total annual costs." This research contributes to advancing the optimization of CRS, offering a promising approach for achieving cost savings and environmental benefits in low-temperature industrial processes.

3. Methodology

The following stages are employed to optimize and prioritize alternatives in complex systems, especially those with conflicting criteria that require a compromise solution. Fig. 1 illustrates the typical steps of the FAG method, which are utilized in this study.

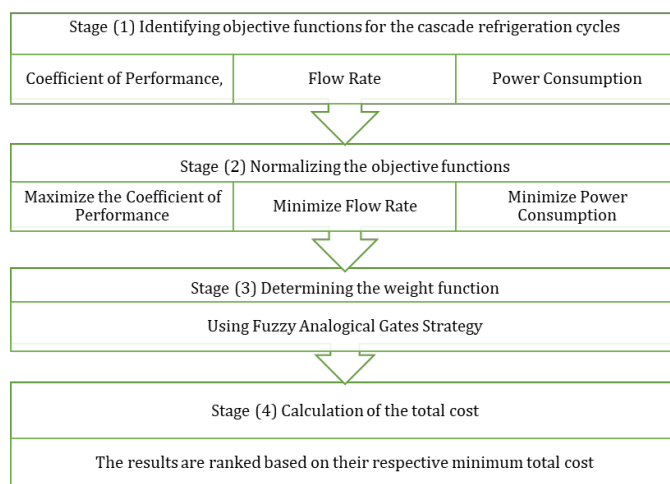


Fig.1. Flow chart of typical steps involved in the FAG approach.

Stage 1: Objective functions identification

A suitable optimization or simulation technique is employed to identify the optimal solution that meets the problem's requirements. The choice of the most appropriate mathematical approach and optimization or simulation method depends on the specific characteristics of the (CRS), and the problem being addressed.

A mathematical model has been formulated using equations from existing literature to inspect both (CRS) and (TCRS) from both thermodynamic and economic perspectives. To streamline and simplify the analysis, assumptions made by Lee *et al.* [11] and Zhili Sun, *et al.* [12-14] were applied.

Before conducting the thermodynamic modelling, the basic assumptions and input parameter values for CRS and TCRS were established as outlined in Table 1.

Based on these assumptions, mass and energy balance are applied to each component to assess the system's overall performance. The equations for all components of CRS and TCRS are compiled in Table 2 which provides a comprehensive summary of these equations.

The total compressor work input for CRS is:

$$W_{Total} = W_{LTC} + W_{HTC} \quad (1)$$

And the total compressor work input for TCRS is

$$W_{Total} = W_{LTC} + W_{MTC} + W_{HTC} \quad (2)$$

The overall COP is given by:

$$COP = \frac{Q_{evap.}}{W_{Total}} \quad (3)$$

Table 1. Basic assumptions for CRS and TCRS cycles.

Parameters	Values	Parameters	Values
$Q_{evap.}$ kW	10	ΔT , °C	2 to 8
η_s , %	80	T_{LC} , °C	-6 to 6
η_m , %	100	Superheating in (LTc), °C	5
$\eta_{elec.}$, %	100	Superheating in (MTc), °C	12
T_D , °C	25	Superheating in (HTc), °C	12
$T_{Cond.}$, °C	37 to 55	ΔT of air, °C	-263.15
CRS $T_{evap.}$, °C	-50 to -21	T_i of air to the evaporator, °C	-10
TCRS $T_{evap.}$, °C	-120 to -180		

Table 2. Thermodynamic modelling/ equations of CRS and TCRS.

Mass and energy balance equations of CRS [13-14]		
Components	Mass balance	Energy balance
Evaporator	$\dot{M}_4 = \dot{M}_1 = \dot{M}_{LTC}$ $\dot{M}_{LTC} = \frac{Q_{evap}}{h_1 - h_4}$	$Q_{evap} = \dot{M}_{LTC} (h_1 - h_4)$
(LTc) compressor	$\dot{M}_1 = \dot{M}_2 = \dot{M}_{LTC}$	$W_{LTC} = \frac{\dot{M}_{LTC} (h_2 - h_1)}{\eta_s * \eta_m * \eta_{elec}}$
Cascade condenser	$\dot{M}_2 = \dot{M}_3 = \dot{M}_{LTC}$ $\dot{M}_8 = \dot{M}_5 = \dot{M}_{HTC}$	$Q_{Cas} = \dot{M}_{LTC} (h_2 - h_3)$ $Q_{Cas} = \dot{M}_{HTC} (h_5 - h_8)$
(LTc) throttle valve	$\dot{M}_3 = \dot{M}_4 = \dot{M}_{LTC}$	$h_3 = h_4$
(HTc) compressor	$\dot{M}_5 = \dot{M}_6 = \dot{M}_{HTC}$	$W_{HTC} = \frac{\dot{M}_{HTC} (h_6 - h_5)}{\eta_s * \eta_m * \eta_{elec}}$
(HTc) throttle valve	$\dot{M}_7 = \dot{M}_8 = \dot{M}_{HTC}$	$h_7 = h_8$
Condenser	$\dot{M}_6 = \dot{M}_7 = \dot{M}_{HTC}$	$Q_{Cond} = \dot{M}_{HTC} (h_6 - h_7)$

Energy balance equations for TCRS [12]		
Component	Temperature cycle	Energy balance
Compressor	High	$W_{HTC,Comp} = \frac{\dot{M}_{HTC}(h_{10} - h_9)}{\eta_{HTC,Comp}} = \dot{M}_{HTC}(h_{10} - h_9)$
Condenser		$Q_{Cond} = \dot{M}_{HTC}(h_{10} - h_{11})$
Throttle valve		$h_{11} = h_{12}$
Compressor	Medium	$W_{MTC,Comp} = \frac{\dot{M}_{MTC}(h_6 - h_5)}{\eta_{MTC,Comp}} = \dot{M}_{MTC}(h_6 - h_5)$
Cascade heat exchanger		$Q_{MTC} = \dot{M}_{MTC}(h_6 - h_7) = \dot{M}_{HTC}(h_9 - h_{12})$
Throttle valve		$h_7 = h_8$
Compressor	Low	$W_{LTC,Comp} = \frac{\dot{M}_{LTC}(h_2 - h_1)}{\eta_{LTC,Comp}} = \dot{M}_{LTC}(h_2 - h_1)$
Cascade heat exchanger		$Q_{LTC} = \dot{M}_{LTC}(h_2 - h_3) = \dot{M}_{MTC}(h_5 - h_8)$
Throttle valve		$h_3 = h_4$
Evaporator		$Q_{evap} = \dot{M}_{LTC}(h_1 - h_4)$

Stage 2: Objective functions normalization

In the pursuit of optimizing cascade refrigeration systems, it becomes imperative to establish quantifiable rules governing the synthesis process. In this manuscript, a synthesis algorithm based on expert rules tailored for economic design problems is proposed. Three key rules guide our approach:

Rule (1): Prioritize configurations with high coefficients of performance (COP), indicating superior energy efficiency.

$$\text{Normalized COP: } \mu_{COP} = \frac{COP - COP_{min}}{COP_{max} - COP_{min}} \quad (4)$$

Rule (2): Favor configurations with lower refrigerant flow rates (\dot{m}), signifying reduced resource consumption. Normalized refrigerant flowrate:

$$\mu_{\dot{M}} = \frac{\dot{M}_{max} - \dot{M}}{\dot{M}_{max} - \dot{M}_{min}} \quad (5)$$

Rule (3): Give precedence to configurations with lower total power consumption of the cycle ($W_{Total\ max}$), indicating greater operational efficiency. Normalized Total power of cycle:

$$\mu_{W_{Total}} = \frac{W_{Total\ max} - W_{Total}}{W_{Total\ max} - W_{Total\ min}} \quad (6)$$

These fuzzy quantities (μ) represent the degree to which each rule is satisfied based on normalized values of COP, refrigerant flow rate, and total power consumption. They operate the expert rules in our synthesis algorithm for economical design problems in cascade refrigeration systems.

Stage 3: Weight function determination using FAG strategy

Our synthesis algorithm leverages a fuzzy analogical gates strategy, executed through a three-step process:

Step 1: Estimate the normalized parameters of the variables, including maximum COP, minimum refrigerant flow rate, and minimum total power of the cycle, using predefined equations (4, 5 and 6).

Step 2: Utilize two sequential fuzzy analogical gates, a symmetric AND gate Fig. 2. (a) followed by an asymmetric Invoke gate Fig. 2. (b) to process the normalized input variables in the network as shown in Fig. 3 [15-16].

Symmetric AND Gate:

$$w = m \otimes n = m[1 - \xi(n, m)] + n[1 - \xi(m, n)] \quad (7)$$

where $\xi(n, m)$ and $\xi(m, n)$ are defined by exponential functions to modulate the relationship between inputs.

$$\xi(n, m) = \exp\left[\frac{an^2 + bnm}{n^2 + m^2}\right] \text{ and } m, n \in R \quad (8)$$

$$\xi(m, n) = \exp \left[\frac{am^2 + bmn}{n^2 + m^2} \right] \text{ and } m, n \in R \quad (9)$$

The parameters **a** and **b** values are 2.28466 and -0.089817, respectively.

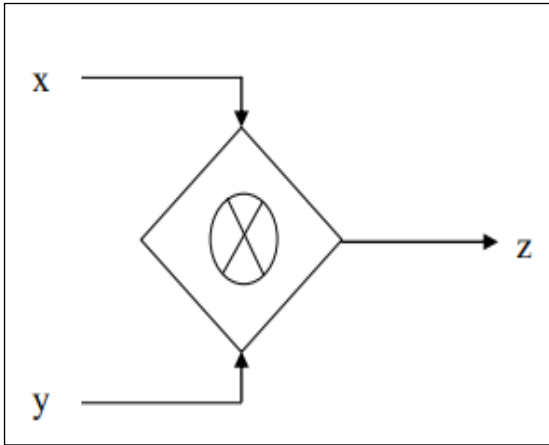


Fig. 2. (a) Symbols for AND gate

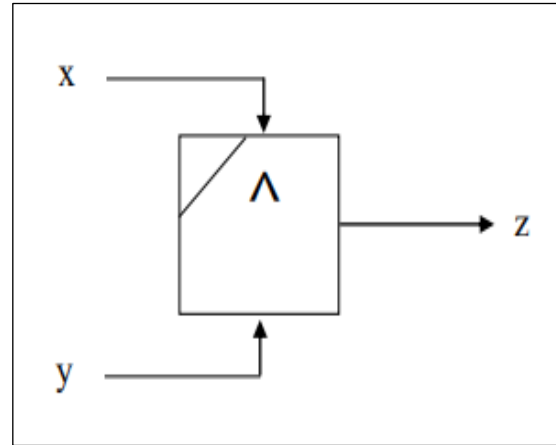


Fig. 2. (b) Symbols for Invoke gate

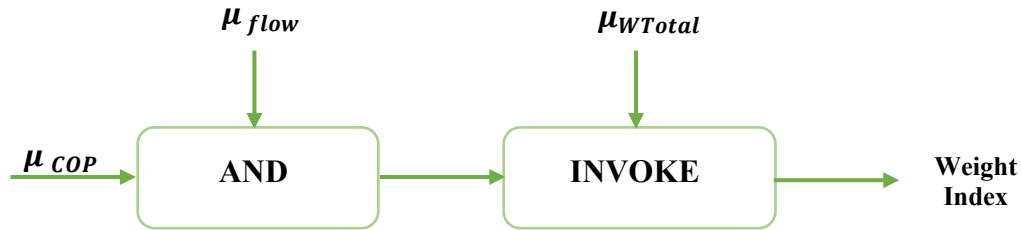


Fig.3. Fuzzy analogical gates network.

Asymmetric Invoke Gate:

$$w = m \wedge n = m\xi_1[(n, m)] + n[1 - \xi_2(m, n)] \quad (10)$$

where $\xi_1(n, m)$ and $\xi_2(m, n)$ are exponential functions defining the fuzzy relation between inputs, with parameters tailored for asymmetry.

$$\xi_1(n, m) = \exp \left[\frac{-(\alpha_1 n^2 + \beta_1 nm)}{n^2 + m^2} \right] \text{ and } m, n \in R \quad (11)$$

$$\xi_2(m, n) = \exp \left[\frac{-(\alpha_2 n^2 + \beta_2 mn)}{m^2 + n^2} \right] \text{ and } m, n \in R \quad (12)$$

where, $(\alpha_1 = 1.4749267, \beta_1 = 0.92870491, \alpha_2 = 2.6317713, \beta_2 = 0.2287955)$

Step 3: Determine the optimal weight index (W.I) by comparing outputs from each gate and selecting the maximum value:

$$W.I_{opt.} = \max\{W.I_1, W.I_2, W.I_3, \dots, W.I_n\} \quad (13)$$

This methodology aims to identify the most efficient configurations of cascade refrigeration systems, enhancing energy utilization and process sustainability. Subsequent sections of this manuscript delve into the theoretical framework, computational methodologies, and practical applications of our proposed synthesis approach, providing insights for designing and operating cascade refrigeration systems across diverse industrial settings.

Stage 4: Total cost calculation

The economic analysis in this study focuses on two main factors: capital cost and operational cost. The succeeding assumptions were adopted for the analysis:

- The equipment's service life was estimated to be 10 years.
- It was assumed that the system operates annually for 7000 hours.
- The electricity cost was estimated to be 0.12 \$/ kilowatt-hour.

- The interest ratio was set at 8%.
- expansion valves cost was neglected in this analysis.

The overall cost C_{Total} is:

$$C_{Total} = T_{CC} + C_{Oper}. \quad (14)$$

3.1. Capital cost

In engineering economics, capital costs are often expressed on an annual basis. The capital cost for a specific year is calculated using (CRF). Cost functions for various components were derived from the research of Mosaffa *et al.* [17] and Aminyavari *et al.* [18]. The capital cost of each component is estimated using the following component-specific cost functions:

$$\text{High temperature circuit compressor cost: } C_{comp,H} = 9624.2 W_{comp,H}^{0.46} \quad (15)$$

$$\text{Low temperature circuit compressor cost: } C_{comp,L} = 10167.5 W_{comp,L}^{0.46} \quad (16)$$

$$\text{High temperature circuit condenser cost: } C_{cond} = 1397 A_{o,cond}^{0.89} \quad (17)$$

$$\text{Low temperature circuit evaporator cost: } C_{Evap.} = 1397 A_{o,Evap.}^{0.89} \quad (18)$$

$$\text{Cascade condenser heat exchanger cost: } C_{Cas,cond} = A_{Cas,cond}^{0.68} \quad (19)$$

The area A_o of each (HX) is expressed as a function of (U_o) and (ΔT) , following Nasruddin [19]:

Evaporator: $A_o = Q/(U_o \cdot \Delta T)$ with $U_o = 18.03 \text{ W/m}^2\text{K}$;

Condenser: $A_o = Q/(U_o \cdot \Delta T)$ with $U_o = 6.85 \text{ W/m}^2\text{K}$

Cascade heat exchanger: $A_o = Q/(U_o \cdot \Delta T)$ with $U_o = 64.87 \text{ W/m}^2\text{K}$

The total capital expenditure:

$$T_{CC} = (C_{comp,H} + C_{comp,L} + C_{cond} + C_{Evap} + C_{Cas,cond}) * CRF \quad (20)$$

The (CRF) converts the present value of capital costs into an annualized form. It is calculated using the formula provided by Mosaffa *et al.* [17] and Navidbakhsh [20].

$$CRF = \frac{l(1+l)^\omega}{(1+l)^\omega - 1} \quad (21)$$

3.2. Operational cost

In addition to capital costs, operational costs related to the power consumption of compressors must also be assessed:

$$C_{Oper.} = (W_{comp,H} + W_{comp,L}) * C_{elec}. \quad (22)$$

4. Case studies

Two cases will be illustrated in the following subsections to demonstrate the applicability of our method, two and three stages of cascade refrigeration structure. Table 3 lists the essential properties of various refrigerants considered in this study.

Table 3. Thermophysical properties of R1270, R1150, R 50, NH₃ and CO₂ refrigerants.

Refrigerant	Molecular weight g/mol	Critical temperature °C	Boling point temperature, °C	CAS Number
R 1270	42.08	92.44	- 47.69	115 – 07 – 1
R1150	28.05	9.166	- 103.7	74–85–1
R50	16.04	- 82.61	- 161.5	74–82–8
NH3	17.03	132.4	- 33.45	7664–41–7
CO2	44.01	30.95	- 78.55	124–38–9

Case 1. Two Stage CRS using NH₃/CO₂ [7]

Figure 4 presents a schematic diagram of a standard (CRS), consisting of two interconnected single-stage vapor compression refrigeration cycles via a (CHX) This specialized (HX) function as a condenser in the (LTc) while also operating as an evaporator in the (HTc). Within the (CHX), Heat released by (LTc) refrigerant is subsequently absorbed by the HTc refrigerant.

In the (LTc) the refrigerant absorbs an amount of heat at an evaporator temperature of $T_{evap.}$ undergoing vaporization. The resulting vapor is compressed by the (LTc) compressor (state 1), increasing its temperature/pressure resulting in state 2. The refrigerant then enters

the CHX, where it releases heat, $Q_{casc.}$ at the (LTc) condenser temperature, T_{LC} . This heat transfer enables the (HTc) refrigerant, operating at the (HTc) evaporator temperature, T_{HE} , to evaporate (state 5) while simultaneously condensing the (LTc) refrigerant (state 3).

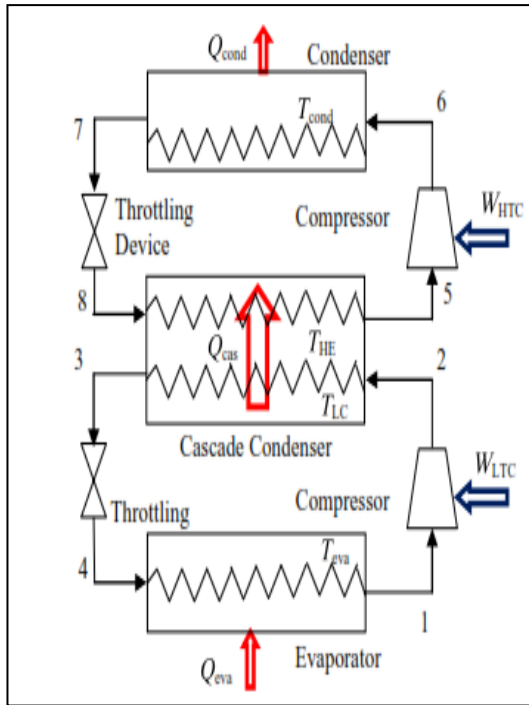


Fig. 4. CRS schematic diagram.

Case 2. Three Stage TCRS using R50/R1150/R1250 [12]

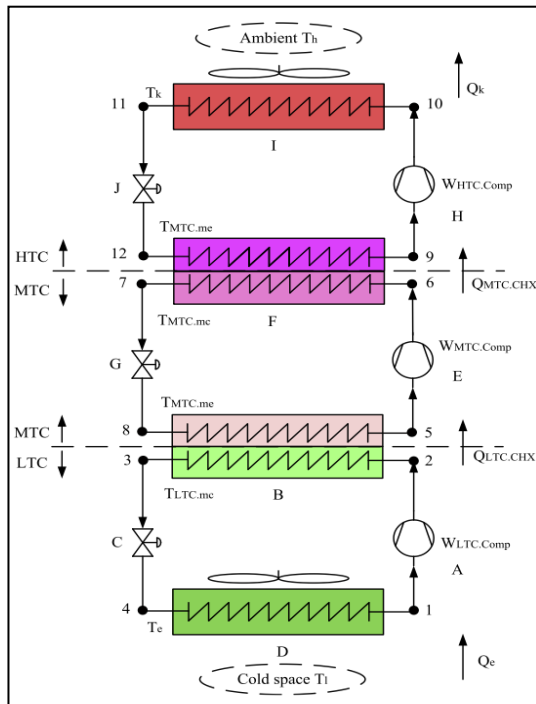


Fig. 5. TCRS Schematic diagram.

After condensation, the (LTc) refrigerant travels through the (LTc) throttle, expanding to the evaporator pressure at state 4 prior to re-entering the evaporator.

Simultaneously, the vaporized (HTc) refrigerant exits the (CHX) and enters the (HTc) compressor, where work input is utilized to elevate the refrigerant pressure up to the condenser level. The pressurized refrigerant, now superheated, goes into the condenser at (state 6), where it undergoes desuperheating and condenses into saturated liquid at (state 7), at $T_{cond.}$, releasing heat, $Q_{cond.}$. The (HTc) refrigerant passes through the (HTc) throttle, expanding to the evaporator pressure at state 8, before circulating back to the (HTc) evaporator. All those key parameters significantly impact the performance and efficiency of the CRS as whole.

A three-stage (TCRS) incorporates three interconnected single tier cooling loops: the high, medium and low temperature cycle. Figure 5 illustrates the schematic diagram of the TCRS. In this system, (LTc) evaporator takes in the cooling load $Q_{evap.}$ from the cold space.

Within the (CHX) of the (LTc), the heat transferred from (MTC) cooling fluid to (LTc) refrigerant equals to the summation of the cooling load taken by the (LTc) evaporator and the power supplied to the (LTc) compressor. Similarly, in the (CHX) of the (MTC), the heat exchange between (MTC) and (HTc) refrigerants equals the summation of the heat transferred by the (LTc) (CHX) and the power consumed by the (MTC) compressor. The condenser expels, Q_H , to the surrounding environment, where Q_H is equal to the combined heat rejected by the (MTC's) (CHX) and the work done by the (HTc) compressor.

5. Results and discussion

The performance of the (CRS) and the (TCRS) were evaluated through a comprehensive parametric study. The key parameters analyzed include the heat load for evaporation and condensation, mass flow rate, compressor input power, and the coefficient of performance (COP).

For CRS: In the first stage of analysis, the impact of varying temperature differences (ΔT) on the Cascade Refrigeration System (CRS) was assessed across several key parameters such as evaporator and condenser heat load where $Q_{evap. 1}$ and 2 remained relatively stable as ΔT increased from 2°C to 8°C, reflecting consistent cooling capacities. The $Q_{Cond.}$ also maintained a constant load of 10 kW throughout, indicating stable heat rejection. The total compressor work input ($W_{comp Total}$) exhibited slight variations, with values ranging from 4.2833 kW at $\Delta T=2^\circ\text{C}$ to 4.5038 kW at $\Delta T=8^\circ\text{C}$. This suggests a modest increase in energy consumption with higher temperature differences as shown in Table 4.

Table 4. Stages results of FAG method for CRS.

Stage 1 results							
$\Delta T, ^\circ\text{C}$	2	3	4	5	6	7	8
$Q_{\text{evaporator } 1} \text{ (kW)}$	6.7875	6.7611	6.7342	6.7069	6.6791	6.6509	6.6222
$Q_{\text{evaporator } 2} \text{ (kW)}$	7.7093	7.6793	7.6488	7.6177	7.5862	7.5541	7.5216
$Q_{\text{condenser}} \text{ (kW)}$	10	10	10	10	10	10	10
$W_{\text{comp } 1} \text{ (kW)}$	1.2291	1.2243	1.2194	1.2145	1.2095	1.2044	1.1992
$W_{\text{comp } 2} \text{ (kW)}$	3.0542	3.0943	3.1350	3.1764	3.2184	3.2612	3.3046
$W_{\text{comp Total}} \text{ (kW)}$	4.2833	4.3186	4.3544	4.3909	4.4279	4.4655	4.5038
\dot{M} of 1 st cycle (kg/h)	80.1531	79.8408	79.5233	79.2006	78.8726	78.5393	78.2008
\dot{M} of 2 nd cycle (kg/h)	21.3761	21.2472	21.1177	20.9876	20.8568	20.7255	20.5935
$\dot{M}_{\text{Tot.}} \text{ (kg/h)}$	101.5292	101.0880	100.6410	100.1882	99.7294	99.2648	98.7942
COP	1.5846	1.5656	1.5465	1.5275	1.5084	1.4894	1.4704
Stages 2 and 3 results							
$\Delta T, ^\circ\text{C}$	$\mu_{\text{COP max}}$		$\mu_{\text{flow min}}$		$\mu_{\text{Power min}}$		W.I
2	1.0000		0.0000		1.0000		0.0000
3	0.8332		0.1613		0.8401		0.0423
4	0.6664		0.3247		0.6774		0.3426
5	0.4996		0.4903		0.5121		0.5290
6	0.3329		0.6581		0.3441		0.3450
7	0.1663		0.8279		0.1734		0.0782
8	0.0000		1.0000		0.0000		0.0000
Stage 4 results							
$\Delta T, ^\circ\text{C}$	TCC (\$/Yr)		TOC (\$/Yr)		Total Cost (\$/Yr)		
2	10057.1		9380.5		19437.60		
3	9838.63		9457.7		19296.31		
4	9702.69		9536.2		19238.88		
5	9603.79		9616.0		19219.79		
6	9525.13		9697.1		19222.23		
7	9458.89		9779.5		19238.40		
8	9400.95		9863.2		19264.17		

\dot{M} of 1st and 2nd cycle decreased progressively with increasing ΔT , resulting in a reduction of $\dot{M}_{Tot.}$ from 101.5292 kg/h to 98.7942 kg/h at $\Delta T=8^\circ\text{C}$. This trend indicates reduced refrigerant mass circulation with higher temperature gradients. The COP of the CRS showed a gradual decline from 1.5846 to 1.4704. This decrease highlights a diminishing efficiency as ΔT increases, necessitating higher energy input for cooling. In stages 2 and 3, optimization metrics such as ($\mu_{COP max}$), ($\mu_{flow min}$), and ($\mu_{Power min}$) were analyzed across different ΔT values. The optimal (W.I) using the FAG method peaked at $\Delta T=5^\circ\text{C}$ with a value of 0.5290, indicating an optimal balance between operational efficiency and energy consumption within the studied range. The cost analysis in stage 4 evaluated the Total Capital Cost (TCC), across varying ΔT values. Total annual costs initially decreased with increasing ΔT , with the lowest total cost observed at $\Delta T=5^\circ\text{C}$. However, beyond $\Delta T=5^\circ\text{C}$, total costs began to rise again. This increase

reflects higher operational expenses associated with greater energy consumption and reduced system efficiency at higher temperature differences.

Table 5. Stages results of FAG method for TCRS.

Stage 1 results							
$\Delta T, ^\circ\text{C}$	2	3	4	5	6	7	8
$Q_{\text{evaporator1}}$ (kW)	4.9803	4.9723	4.9736	4.9689	4.9592	4.9453	4.9279
$Q_{\text{evaporator2}}$ (kW)	6.2633	6.2738	6.2755	6.2695	6.2574	6.2398	6.2179
$Q_{\text{evaporator3}}$ (kW)	7.6453	7.6716	7.6874	7.6943	7.6939	7.6872	7.6753
$Q_{\text{condenser}}$ (kW)	10	10	10	10	10	10	10
$W_{\text{comp 1}}$ (kW)	1.2830	1.3016	1.3019	1.3007	1.2981	1.2945	1.2899
$W_{\text{comp 2}}$ (kW)	1.3819	1.3978	1.4119	1.4248	1.4365	1.4474	1.4574
$W_{\text{comp 3}}$ (kW)	2.3547	2.328	2.3126	2.3057	2.3061	2.3128	2.3247
$W_{\text{comp Total}}$ (kW)	5.0197	5.0277	5.0264	5.0311	5.0408	5.0547	5.0721
\dot{M} of 1 st cycle (kg/h)	38.3812	37.4610	37.4709	37.1101	37.3626	37.2578	37.1267
\dot{M} of 2 nd cycle (kg/h)	48.1613	48.1277	48.0272	47.5125	47.6663	47.4233	47.1488
\dot{M} of 3 rd cycle (kg/h)	109.5296	104.4507	100.0899	96.1222	92.9953	89.8613	87.1189
$\dot{M}_{\text{Tot.}}$ (kg/h)	196.0721	190.0394	185.5880	180.7448	178.0242	174.5424	171.3944
COP_1	3.8818	3.8203	3.8203	3.8203	3.8203	3.8203	3.8203
COP_2	4.5323	4.4884	4.4446	4.4003	4.3559	4.3112	4.2663
COP_3	3.2468	3.2949	3.3242	3.3371	3.3363	3.3237	3.3016
$\text{COP}_{\text{Total}}$	0.9922	0.9890	0.9895	0.9876	0.9838	0.9784	0.9716
Stages 2 and 3 results							
$\Delta T, ^\circ\text{C}$	$\mu_{\text{COP max}}$	$\mu_{\text{flow min}}$		$\mu_{\text{Power min}}$		W.I	
2	1.0000	0.0000		1.0000		0.0000	
3	0.8449	0.2445		0.8462		0.1277	
4	0.8700	0.4248		0.8712		0.4501	
5	0.7790	0.6211		0.7807		0.7293	
6	0.5947	0.7313		0.5972		0.6661	
7	0.3295	0.8724		0.3318		0.2884	
8	0.0000	1.0000		0.0000		0.0000	
Stage 4 results							
$\Delta T, ^\circ\text{C}$	TCC (\$/Yr)		TOC (\$/Yr)		Total Cost (\$/Yr)		
2	257468.1		439716.9		697185.0		
3	256491.6		440427.7		696919.3		
4	256131.5		440313.2		696444.8		
5	255531.3		440728.5		696259.9		
6	254787.0		441571.5		696358.6		
7	253897.5		442790.5		696688.2		
8	252896.0		444307.2		697203.2		

The following observations were made for the first stage: The evaporator heat loads $Q_{\text{evap.}}$ and the condenser heat load $Q_{\text{cond.}}$ remained stable across different temperature differences (ΔT). The total compressor work input showed slight variations, with the highest being 5.0721 kW at $\Delta T=8^\circ\text{C}$. The total mass flow rate \dot{M} decreased as ΔT increased, from 196.0721 kg/h to 171.3944 kg/h. The overall COP displayed a slight decrease, from 0.9922 at $\Delta T=2^\circ\text{C}$ to 0.9716 at $\Delta T=8^\circ\text{C}$. For the 2nd and 3rd stages Results, the key performance metrics were analyzed and show that the $\mu_{\text{COP max}}$ decreased from $\Delta T=2^\circ\text{C}$ to $\Delta T=8^\circ\text{C}$ $\mu_{\text{flow min}}$ and $\mu_{\text{Power min}}$ exhibited increasing trends with increasing ΔT . The optimum W.I is the highest value and equal to 0.7293 at $\Delta T=5^\circ\text{C}$. For the final stage, the cost analysis results showed that the total cost per year decreased slightly with increasing ΔT from \$697,185.0 at $\Delta T=2^\circ\text{C}$ to \$696,259.9.2 at $\Delta T=5^\circ\text{C}$ and start increasing again to reach \$697,203.2 at $\Delta T=8^\circ\text{C}$. Previous studies have indicated that the optimum intermediate temperature ranges between 2 to 8°C . The optimum intermediate temperature obtained in this study was at $\Delta T=5^\circ\text{C}$, which corresponds with the FAG results and cost analysis as show in Table 5. The parametric study provides significant insights into the performance optimization of both CRS and TCRS.

5.1. Performance analysis

COP Variations: The COP showed a consistent trend of decreasing with increasing temperature difference. This is indicative of reduced system efficiency at higher ΔT . The highest COP values were observed at lower ΔT , highlighting the importance of maintaining a lower temperature difference for enhanced system performance.

Compressor Work Input: The total work input for the compressors increased slightly with increasing ΔT , impacting the overall energy efficiency of the system. This suggests a need for optimizing compressor operations to minimize energy consumption.

Mass Flow Rate: The mass flow rate trends suggest that higher ΔT results in lower refrigerant flow rates, which could affect the cooling capacity. Therefore, maintaining an optimal ΔT is crucial for balancing flow rates and achieving desired cooling performance.

Cost Implications: The total cost analysis revealed that while the operational costs remained relatively stable, there were marginal cost increases at higher ΔT . This underscores the importance of cost-effective temperature management to ensure economic viability of the refrigeration systems.

System Design Recommendations: It is recommended to operate the CRS and TCRS at lower temperature differences to maximize COP and minimize energy consumption. Enhancements in compressor efficiency and precise control of refrigerant flow rates are critical for improving overall system performance.

A balance between operational efficiency and cost-effectiveness must be achieved by optimizing key parameters such as ΔT , compressor work input, and mass flow rates.

Overall, the findings from this study offer valuable guidelines for designing and operating cascade refrigeration systems with improved performance and cost efficiency.

6. Conclusion

This study provides an in-depth parametric analysis of (CRS) and (TCRS) using the Fuzzy Analogical Gates (FAG) method. Key performance indicators such as the coefficient of performance (COP), compressor input power, mass flow rates, and total cost per year were meticulously evaluated with varying temperature differences (ΔT).

Key findings and benefits:

- **COP optimization:** The study demonstrates that the COP decreases with increasing ΔT . Maintaining a lower ΔT significantly enhances system efficiency, providing a more energy-efficient operation.
- **Energy consumption:** There is a slight increase in compressor work input with higher ΔT , indicating that optimized temperature control can lead to substantial energy savings.
- **Refrigerant flow management:** The analysis shows a decrease in mass flow rates with higher ΔT , suggesting that optimal ΔT values are crucial for maintaining adequate cooling capacity and ensuring system reliability.
- **Cost efficiency:** The cost analysis indicates marginal increases in operational costs at higher ΔT , underscoring the economic benefit of maintaining lower temperature differences to balance performance and cost.
- **Optimum intermediate temperature:** The optimum intermediate temperature was found to be at $\Delta T=5^\circ\text{C}$, which aligns with the FAG results and cost analysis, confirming it as the most efficient and cost-effective operational point.

Implications:

The findings emphasize the importance of optimizing key operational parameters to achieve higher efficiency and cost-effectiveness in CRS and TCRS. By maintaining lower temperature differences, improving compressor efficiency, and accurately controlling refrigerant flow rates, these systems can achieve enhanced performance and economic viability.

Future work directions:

1. **Advanced control strategies:** Future research could explore the development and implementation of advanced control algorithms to dynamically optimize ΔT , further improving system efficiency and responsiveness.

2. Integration with renewable energy: Investigating the integration of renewable energy sources such as solar or wind power could provide a sustainable and cost-effective energy supply for CRS and TCRS, reducing the overall environmental impact.
3. Material and design innovations: Exploring new materials and innovative design approaches for key components like compressors and heat exchangers can lead to improvements in system performance and longevity.
4. Real-Time monitoring and diagnostics: Implementing real-time monitoring and diagnostic tools to predict and prevent potential failures could enhance system reliability and reduce maintenance costs.

In conclusion, the insights gained from this study provide valuable guidelines for the design, operation, and optimization of efficient and cost-effective refrigeration systems. The benefits highlighted in terms of energy savings, cost efficiency, and system reliability underscore the potential for significant advancements in the field of refrigeration technology.

Author Contributions: **Mohamed A. Atef:** Writing – original draft, Resources, Software, Investigation, Analysis. **Shazly M. Salem:** Conceptualization, Editing, Resources & Supervision. **Mostafa H. Hussein:** Conceptualization, Resources, Writing – original draft, Methodology, Investigation, Validation, Writing – review, Editing & Supervision.

Declaration of competing interest: The authors declare that they have no known competing financial interests or personal relationships that could have appeared to influence the work reported in this paper.

Funding information: This research did not receive any specific grant from funding agencies in the public, commercial, or non-profit sectors.

Glossary

MINLP	<i>mixed-integer nonlinear programming.</i>
GDP	<i>generalized disjunctive programming.</i>
GA	<i>genetic algorithm</i>
HENs	<i>heat exchanger networks.</i>
PSO	<i>Particle swarm optimization</i>
SA	<i>simulated annealing</i>
HX	<i>Heat exchanger</i>
CRS	<i>Cascade Refrigeration System</i>
TCRS	<i>Three-Stage Cascade Refrigeration System</i>
Comp	<i>Compression Process or Compressor</i>
TV	<i>Throttling Process or Throttle Value</i>
Evap.	<i>Evaporation Process or Evaporate</i>
Cond.	<i>Condensation Process or Condenser</i>
CHX	<i>Cascade Heat Exchanger or Heat Transfer of Condensing Evaporator</i>

Abbreviations

List of symbols

A_o	<i>Area in m²</i>
C	<i>Capital cost/ Cost rate</i>
COP	<i>Coefficient of performance</i>
CRF	<i>Capital recovery factor</i>
E	<i>Annual energy consumption</i>
h	<i>Enthalpy</i>
(HTc)	<i>High-temperature circuit/cycle</i>
(LTc)	<i>Low-temperature circuit/cycle</i>
(MTc)	<i>Medium temperature circuit/cycle</i>
I	<i>Interest rate</i>
FAG	<i>Fuzzy Analogical gates.</i>
$LMTD$	<i>Logarithmic mean temperature difference</i>
\dot{M}	<i>Mass flow rate</i>
$\dot{M}_{Tot.}$	<i>Total Mass flow rate</i>
ω	<i>Plant life</i>

N	Annual operational hour
S	Entropy
T	Temperature
U_o	Overall heat transfer coefficient
W	Work input
ΔT	Temperature Difference
Q	Heat load

Greek symbols

η	Efficiency
μ	key performance metrics

Subscripts

<i>casc.</i>	Cascade condenser
<i>comp,h</i>	(HTc) Compressor
<i>comp,l</i>	(LTc) Compressor
<i>cond.</i>	Condenser
<i>elec.</i>	Electrical
<i>evap.</i>	Evaporator
<i>exp,h</i>	(HTc) Expansion valve
<i>exp,l</i>	(LTc) Expansion valve
<i>m</i>	Mechanical
<i>s</i>	Isentropic

References

- [1] Barnés FJ, and King CJ. Synthesis of cascade refrigeration and liquefaction systems. *Ind. Eng. Chem. Process Des. Dev.*, 1974; 13(4): 421–433.
<https://doi.org/10.1021/i260052a022>
- [2] Cheng WB, and Mah RSH. Interactive synthesis of cascade refrigeration systems. *Ind. Eng. Chem. Process Des. Dev.*, 1980; 19(3): 410–420.
<https://doi.org/10.1021/i260075a015>
- [3] Zhang J, and Xu Q. Cascade refrigeration system synthesis based on exergy analysis. *Comput. Chem. Eng.*, 2011; 35(9): 1901–1914.
<https://doi.org/10.1016/j.compchemeng.2011.02.015>
- [4] Dinh H, Zhang J, and Xu Q. Process synthesis for cascade refrigeration system based on exergy analysis. *AIChE J.*, 2015; 61(8): 2471–2488.
<https://doi.org/10.1002/aic.14843>
- [5] Eini S, Shahhosseini HR, Javidi M, Sharifzadeh M, and Rashtchian D. Inherently safe and economically optimal design using multi-objective optimization: The case of a refrigeration cycle. *Process Saf. Environ. Prot.*, 2016; 104: 254–267.
<https://doi.org/10.1016/j.psep.2016.09.010>
- [6] Chen D, Ma X, Luo Y, Ma Y, and Yuan X. Synthesis of refrigeration system based on generalized disjunctive programming model. *Chinese J. Chem. Eng.*, 2018; 26(8): 1613–1620.
<https://doi.org/10.1016/j.cjche.2017.10.017>
- [7] Roy R, and Mandal BK. Thermo-economic analysis and multi-objective optimization of vapour cascade refrigeration system using different refrigerant combinations: A comparative study. *J. Therm. Anal. Calorim.*, 2020; 139: 3247–3261.
<https://doi.org/10.1007/s10973-019-08710-x>
- [8] Chen D, Luo Y, and Yuan X. Refrigeration system synthesis based on de-redundant model by particle swarm optimization algorithm. *Chinese J. Chem. Eng.*, 2022; 50: 412–422.
<https://doi.org/10.1016/j.cjche.2022.06.007>
- [9] Martinelli M, Elsidio C, Grossmann IE, and Martelli E. Simultaneous synthesis and optimization of refrigeration cycles and heat exchangers networks. *Appl. Therm. Eng.*, 2022; 206: 118052.
<https://doi.org/10.1016/j.applthermaleng.2022.118052>
- [10] D Chen, Y Luo, and X. Yuan Cascade refrigeration system synthesis based on hybrid simulated annealing and particle swarm optimization algorithm. *Chinese J. Chem. Eng.*, 2023; 58: 244–255.
<https://doi.org/10.1016/j.cjche.2022.10.021>

- [11] Lee T-S, Liu C-H, and Chen T-W. Thermodynamic analysis of optimal condensing temperature of cascade-condenser in CO₂/NH₃ cascade refrigeration systems. *Int. J. Refrig.*, 2006; 29(7): 1100–1108.
<https://doi.org/10.1016/j.ijrefrig.2006.03.003>
- [12] Z Sun, Q Wang, B Dai, M Wang, and Z. Xie Options of low Global Warming Potential refrigerant group for a three-stage cascade refrigeration system. *Int. J. Refrig.*, 2019; 100: 471–483.
<https://doi.org/10.1016/j.ijrefrig.2018.12.019>
- [13] JU Ahamed, R Saidur, and HH. Masjuki A review on exergy analysis of vapor compression refrigeration system. *Renew. Sustain. Energy Rev.*, 2011; 15(3): 1593–1600.
<https://doi.org/10.1016/j.rser.2010.11.039>
- [14] HC Bayrakçı and AE. Özgür Energy and exergy analysis of vapor compression refrigeration system using pure hydrocarbon refrigerants. *Int. J. Energy Res.*, 2009; 33(12): 1070–1075.
<https://doi.org/10.1002/er.1538>
- [15] Hussein MH, Moselhy H, Aly S, and Awad ME. Fuzzy Analogical Gates Approach for Heat Exchangers Networks. *Int. J. Comput. Appl.*, 2013; 73(21): 1-8.
<https://doi.org/10.5120/13015-9646>
- [16] Ibrahim AH, Awad ME, Aly S, Hussein MH. Synthesis and Design of Natural Gas Transmission Networks through Fuzzy Analogical Gates. *Petroleum & Coal*, 2024; 66(2): 665-675.
- [17] Mosaffa AH, Farshi LG, Ferreira CAI, and Rosen MA. Exergoeconomic and environmental analyses of CO₂/NH₃ cascade refrigeration systems equipped with different types of flash tank intercoolers. *Energy Convers. Manag.*, 2016; 117: 442–453.
<https://doi.org/10.1016/j.enconman.2016.03.053>
- [18] Aminyavari M, Najafi B, Shirazi A, and Rinaldi F. Exergetic, economic and environmental (3E) analyses, and multi-objective optimization of a CO₂/NH₃ cascade refrigeration system. *Appl. Therm. Eng.*, 2014; 65(1–2): 42–50.
<https://doi.org/10.1016/j.applthermaleng.2013.12.075>
- [19] Nasruddin N, Arnas A, Faqih A, and Giannetti N. Thermoeconomic optimization of cascade refrigeration system using mixed carbon dioxide and hydrocarbons at low temperature circuit. *Makara J. of Tech.*, 2016; 20(3): 132–138.
<https://doi.org/10.7454/mst.v20i3.3068>
- [20] Navidbakhsh M, Shirazi A, and Sanaye S. Four E analysis and multi-objective optimization of an ice storage system incorporating PCM as the partial cold storage for air-conditioning applications. *Appl. Therm. Eng.*, 2013; 58(1–2): 30–41.
<https://doi.org/10.1016/j.applthermaleng.2013.04.002>

To whom correspondence should be addressed: Mostafa H. Hussein, Chemical Engineering Department, Higher Institute of Engineering – Shorouk Academy- Shorouk City 11837 – Cairo – Egypt, E-mail: theproftifa@gmail.com